AIAA 80-1696R

An Interplanetary Targeting and Orbit Insertion Maneuver Design Technique

Gerald R. Hintz*
Jet Propulsion Laboratory, California Institute of Technology, Pasadena, Calif.

Selecting a planetary encounter aimpoint and a spacecraft propulsive maneuver strategy usually involves tradeoffs of many competing factors. This paper describes such a tradeoff process and its application to the Pioneer Venus Orbiter mission. The method uses parametric data spanning a region of acceptable targeting aimpoints in the delivery space, plus geometric considerations. Trajectory redesign features exercised in flight illustrate the insight made available in solving the interplanetary targeting and orbit insertion maneuver problems. Real-time maneuver adjustments accounted for known attitude control errors, orbit determination updates, and late changes in a targeting specification. An elementary maneuver reconstruction technique is also considered.

Nomenclature

$\vec{B}$ = target parameter in delivery space which is the vector in the $\hat{R}$, $\hat{T}$ plane from the center of the target body to the approach asymptote of the interplanetary trajectory
B plane = $\hat{R}$, $\hat{T}$ plane
ELA = Earth look angle (between the positive spin axis and the spacecraft-to-Earth vector)
E − xd(E − xh) = x days (hours) before Venus encounter at closest approach
HGA = high-gain antenna
h_p = periapsis altitude in the elliptic orbit
i = orbit inclination
OD = orbit determination
P = orbit period
PVO = Pioneer Venus Orbiter
$\hat{R}$ = unit reference vector defined as $\hat{R} = \hat{S} \times \hat{T}$
SLA = Sun look angle (between the positive spin axis and the spacecraft-to-sun vector)
$\hat{S}$ = unit reference vector along incoming approach asymptote
$\hat{T}$ = unit reference vector parallel to ecliptic 1950.0 plane and orthogonal to the $\hat{S}$
TCA = time of closest approach on the hyperbolic trajectory
TCM = trajectory correction maneuver
TCMi = ith interplanetary trajectory correction maneuver
t_{ign} = time of motor ignition
$\vec{V}$ = spacecraft velocity vector
V_∞ = hyperbolic excess velocity
VOI = Venus orbit insertion
$\overline{\Delta V}$ = velocity increment vector
θ = orientation angle of the $\vec{B}$ in the B plane (measured clockwise from the $\hat{T}$)
σ = standard deviation
σ_B(OD) = standard deviation of the OD uncertainty along the $\vec{B}$ (This value can be viewed geometrically as the projection of the 1σ OD ellipse onto the mean $\vec{B}$.)

Coordinate system: All vectors are in the Earth mean ecliptic and equinox of 1950.0 coordinate system. The adjective "celestial" refers to this reference frame.

Presented as Paper 80-1696 at the AIAA/AAS Astrodynamics Conference, Danvers, Mass., Aug. 11-13, 1980; submitted Sept. 16, 1980.

*Member of the Technical Staff. Member AIAA.

Introduction

TO navigate a spacecraft to a planet, an aimpoint must be selected at the target body. The process of selecting a trajectory aimpoint usually involves tradeoffs of several competing factors such as scientific geometry and timing requirements, attitude control needs for celestial reference directions, communication and hardware constraints, and the ever-present desire to conserve fuel. This paper describes such a tradeoff process and the associated spacecraft propulsive maneuver strategy that was developed for the Pioneer Venus Orbiter (PVO) mission.

The PVO mission[1] was designed to take in situ and remote measurements of Venus and its environs. After the launch of the spin-stabilized spacecraft on May 20, 1978, three trajectory correction maneuvers (TCM's) were performed during the interplanetary cruise to achieve the correct arrival time and aimpoint at Venus. On Dec. 4, 1978, a solid rocket was ignited to transfer the spacecraft into a planetary orbit that met the specifications of the onboard experiments and tracking requirements.[2] Additional TCM's were then performed to remove safety biases in the targeted values for the planetary orbit and the effects of orbit determination and execution errors experienced at the Venus orbit insertion (VOI) maneuver. All TCM's, other than the VOI, were performed by an engine fueled with liquid hydrazine.

The technique defined in this paper is illustrated by its application to the PVO mission in the end-to-end determination of the interplanetary trajectory targeting and orbit insertion maneuver strategy design. This process included the preflight candidate launch date analyses, in-flight redesign to accommodate a change in the scientific requirements, real-time maneuver parameter updates for orbit insertion, and performance analysis after maneuver execution.

Preflight Aimpoint Selection Strategy

Targeting Requirements

For the PVO mission, onboard experiments and tracking requirements specified three parameters of the spacecraft orbit about Venus ($P \cong 24$ h, $h_p = 350$ km, $i = 105$ deg) and the epoch of the initial periapsis passage[2] (16 h:00 min:00 s, UTC, on Dec. 4, 1978). Hence, the delivery conditions at Venus had to be such that the solid rocket engine could be used to deliver the spacecraft into an orbit having these specified parameter values. The velocity increment magnitude to be imparted by the insertion motor was fixed in the sense that, once the engine was ignited, it had to burn all the solid rocket fuel. The 350-km periapsis altitude provided a safety bias to account for orbit determination uncertainties experienced at the last interplanetary TCM. Later orbit trim

maneuvers, i.e., TCM's in planetary orbit, would reduce h_p to about 150 km.[2,3]

Interplanetary missions are targeted to the delivery B space (B, θ, TCA) centered at the target body. For each candidate launch date, there is a region in the B plane at Venus in which the spacecraft could achieve the three specified orbit parameter values. The target point was selected before launch from this region as a tradeoff of the following set of objectives: 1) to maximize the celestial latitude of the achieved periapsis vector; 2) to acquire a bright reference star while in the attitude established for the orbit insertion maneuver (That is, it was desired that a bright star, e.g. Arcturus or Capella, be in the field of view of the star sensor for use in determining precisely which attitude had been achieved.); 3) to minimize the use of liquid fuel on the orbiter in order to extend mission life; 4) to reduce the statistical errors in the postinsertion orbit elements; and 5) to provide communications over the high-gain antenna (HGA) while in the insertion attitude, excluding the time the spacecraft was occulted by Venus. The communication constraint was that the Earth look angle (ELA) satisfy 75 deg $<$ ELA $<$ 105 deg.

The spacecraft's thermal design also introduced a pointing requirement for the orbit insertion maneuver.[2] This constraint on the sun look angle (SLA) was checked but was not restrictive in the analysis that follows.

Acceptable Targeting Region

Figure 1 shows the region in the B plane from which the PVO could insert into a satisfactory elliptic orbit after a May 20, 1978 launch. This figure was determined by performing a 3×3 numerical search in targeting a simulated VOI maneuver to P, h_p, and i, using ignition time and the two orientation parameters as controls at each of a selected set of grid points (B_i, θ_j).

The lines at the upper and lower edges of the region in Fig. 1 are essentially h_p constraint boundaries. That is, for points below $\Delta B = -116$ km, it is impossible to insert the spacecraft into a 24-h elliptic orbit having $h_p = 350$ km, using 1.0982 km/s. For points above $\Delta B = 150$ km, it is impossible to decrease the closest approach point to 350 km with the fixed ΔV. Therefore, it would be necessary to accept an h_p value that is too small for trajectories having $\Delta B < -116$ km and one that is too large for $\Delta B > 150$ km. The resulting periapsis altitude error is determined by the focusing factor $\partial h_p / \partial B = 0.6$. The curves on the sides are inclination constraints since they show the amount of θ error that can be corrected to achieve the nominal value $i = 105$ deg, using the available ΔV. Errors in θ outside this region result in an approximate one-to-one loss in inclination since $\partial i / \partial \theta \cong -1.0$ for θ near -105.9 deg.

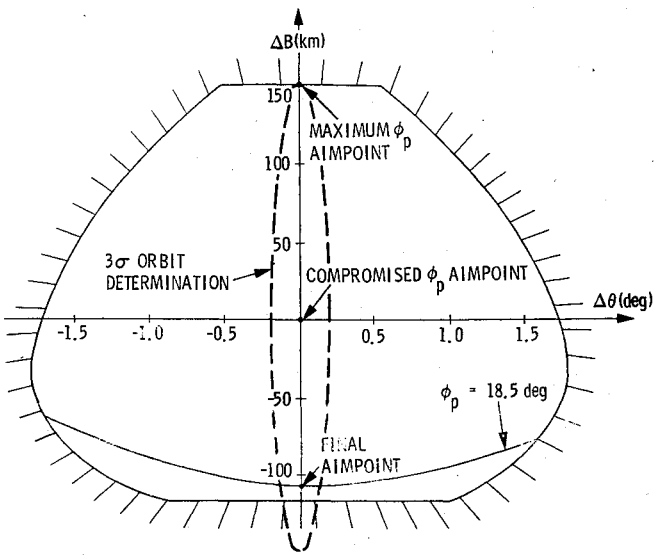

Fig. 1 Acceptable targeting region in the B plane. (Note: the origin is at the preflight aimpoint having $B = 18{,}975.1$ km; $\theta = -105.9$ deg.)

Figure 2 shows contours for the achieved value of the celestial latitude of the in-orbit periapsis vector that correspond to vertical slices in this region in the B plane. Each contour shows the achieved periapsis latitude as a function of ΔB for a fixed value of $\Delta\theta$. Contours for other selected parameters [for example, the three controls, the nontargeted classical orbit elements, the communications angle (ELA), and the sun reference angle (for thermal constraints)] were also generated. Thus, we obtained a complete picture of the orbit insertion maneuver and resulting orbit parameters with variations in the approach trajectory.

Hyperbolic and elliptic trajectories might intersect twice. A $\overline{\Delta V}$ to transfer between these trajectories can be computed for each of these points. When the maneuver is simulated with the fixed ΔV, two transfers might still be available to attain the specified target values, but the elliptic orbits produced by maneuvers at the two points will usually differ from each other. All data given here are for the maneuver at the earlier transfer point unless the text states otherwise.

Aimpoint Selection Strategies

Five candidate launch dates (May 20, 21, 22, 24 and June 1) were analyzed. Figure 2 shows that the celestial latitude of the in-orbit periapsis vector would be maximized at $\Delta B = 150$ km and $\Delta\theta = 0$ deg for the actual launch date of May 20. Table 1 gives the corresponding aimpoint (B, θ), together with the spacecraft controls and ELA for the insertion burn.

Figure 3 shows which reference stars would be in the field of view of the star sensor for each insertion attitude. (The reference star regions were obtained from a NASA Ames document[4] and data obtained from J.R. Cowley Jr.) For example, Arcturus is in the field of view for all orientations above the boundary labeled with the star's name. Contours for the celestial latitude and longitude of the orbit insertion maneuver $\overline{\Delta V}$ were used to determine which arrival points (B, θ) acquired an acceptable reference star as shown in Fig. 3. Communication and thermal constraints were also checked in this manner.

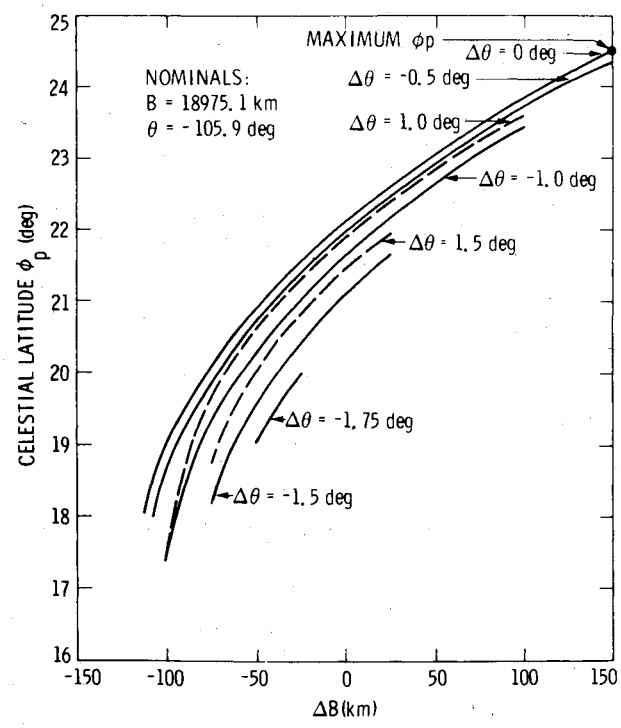

Fig. 2 Achieved latitude of periapsis contours in the B plane.

Table 1 Strategy variations for May 20, 1978 launch

	Maximum ϕ_p	Compromised ϕ_p	$\phi_p = 18.5$ deg
B, km	19,125.1	18,975.1	18,866.8
θ, deg	−105.9	−105.9	−105.9
Altitude at TCA, km	483.8	392.3	326.0
Celestial latitude of $\overline{\Delta V}$, deg	75.0	75.0	74.0
Celestial longitude of $\overline{\Delta V}$, deg	289.0	289.0	313.0
Time of ignition (after TCA), s	253.8	60.7	−118.5
Earth look angle, deg	96.1	96.1	89.9
Sun look angle,[a] deg	76.7	76.7	79.5

[a] Other parameters which did not change with the strategy are: $V_\infty = 3.625$ km/s, $\Delta V = 1.0982$ km/s, and TCA = 16 h:00 min:00 s, UTC on Dec. 4, 1978.

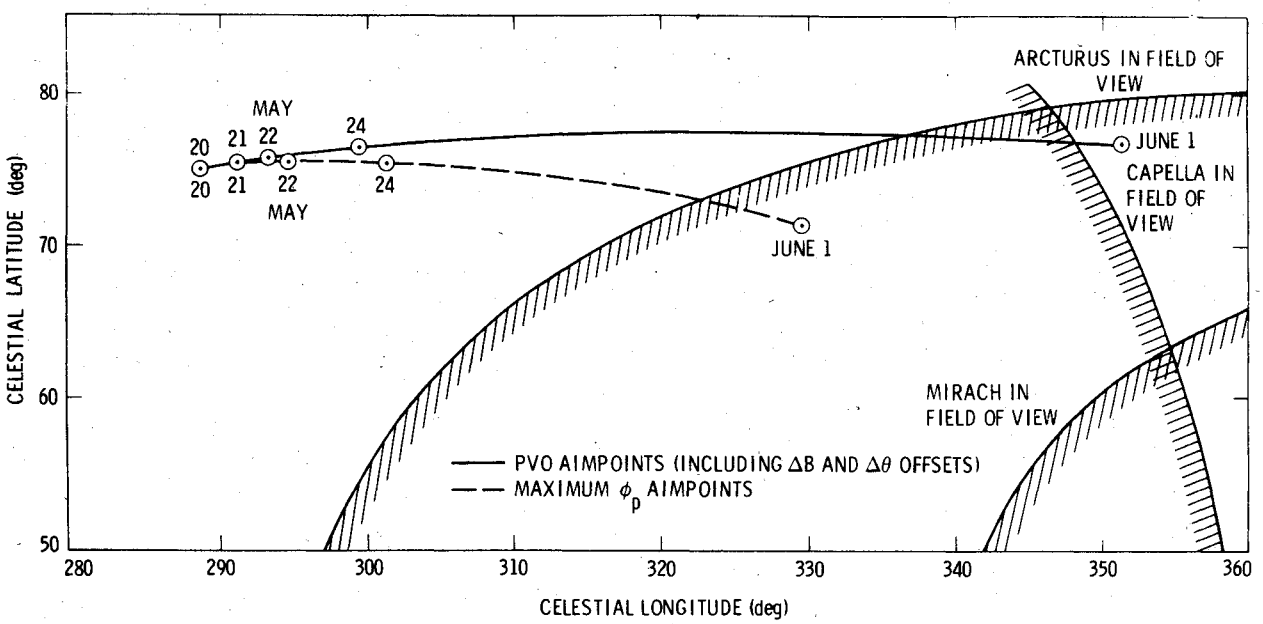

Fig. 3 Reference star candidates for given insertion attitudes.

For early launch dates, the aimpoint which maximized ϕ_p satisfied both the reference star and HGA communication constraints, while achieving the three target parameters. Also, the altitude at hyperbolic closest approach was greater than the 350 km safety value for all of the candidate launch dates.

The maximum ϕ_p maneuver is essentially in-plane and standing up at a small angle to the north ecliptic pole. It is performed after closest approach on the hyperbolic trajectory. Thus, the ϕ_p has been maximized by increasing the value of B to the largest value that permits inserting into a 350-km h_p orbit.

Now consider the best estimate trajectory at the last interplanetary TCM (denoted as TCM3) for the May 20 launch. For an aimpoint at the upper edge of the acceptable targeting region, 50% of the points in the 3σ orbit determination ellipse centered at the maximum ϕ_p aimpoint have a larger than nominal value for B. If the spacecraft were in this half of the ellipse, TCM3 would transfer it to a trajectory that was so high in B that it would be impossible to design a VOI maneuver to achieve an h_p of 350 km. Consequently, for this aimpoint, we would have a high probability of violating our targeting requirements and PVO fuel would be required for additional h_p reduction, violating objective 3. Therefore, an offset

$$\Delta B = -3\sigma_B(\mathrm{OD}) = -150\ \mathrm{km}$$

was introduced along the $\bar{B}$ direction in the aimpoint selection process, according to a preflight estimate of 50 km for σ_B(OD) at TCM3. Thus, we obtained the compromised ϕ_p aimpoint shown in Fig. 1 and the second column of Table 1. The resulting decrease in ϕ_p of about 2.2 deg for all launch dates examined was considered to be an acceptable compromise.

However, as the launch date is delayed, the nominal $\overline{\Delta V}$ orientation moves outside the region that would allow acquiring Arcturus (see Fig. 3). The solution to this problem was to change the aimpoint θ value and perform a VOI maneuver having a slightly larger out-of-plane component. Increasing θ by only 0.9 deg would move the $\overline{\Delta V}$ into the Capella region for a June 1 launch. The resulting loss in ϕ_p would be nil.

The expected 3σ dispersions in the post-VOI elliptic orbit parameters were shown to be acceptable. The execution errors used in the analyses were obtained from Barker et al.[5] and consist of a 1σ pointing error of 0.24 deg and ΔV magnitude of 0.2%. Checking the appropriate contours shows that the ELA and SLA were also satisfactory.

Therefore, the aimpoint strategy for the May 20 through June 1 launches can be summarized as 1) an offset of $-3\sigma_B$(OD) to decrease the target B value from that of the maximum ϕ_p strategy and 2) an offset in the θ value, if necessary. The first two interplanetary TCM's corrected the trajectory to this compromised ϕ_p aimpoint, but later events required a change in this targeting policy for TCM3.

Preflight Venus Orbit Insertion Strategy

Thus, preflight analyses provided an aimpoint at Venus and the associated nominal VOI maneuver. Following the last interplanetary TCM, the VOI strategy would target to the

three specified values, using the three control parameters available at VOI. Thus, the orbit insertion maneuver could correct the orbit determination (OD) and execution errors experienced at the last TCM. The VOI maneuver parameters would then be slightly different from the nominal controls shown in Table 1.

In-Flight Aimpoint Selection Strategy

Angle-of-Attack Problem

The angle of attack is the angle between the spacecraft velocity vector and its positive spin axis. After TCM2, the expected value for this parameter at periapsis in the elliptic orbit was discovered to be too large for the Retarding Potential Analyzer (RPA) experiment, while a lower ϕ_p was seen to produce a satisfactory condition. The preflight PVO aimpoint would produce a celestial latitude of the in-orbit periapsis vector of 22.1 deg and a resulting angle of attack at periapsis of 29 deg. The positive spin axis was tipped slightly away from the south ecliptic pole, but it could not be moved further from this pole because of constraints imposed by the Ultraviolet Spectrometer and Infrared Radiometer experiments. Therefore, reducing the angle of attack required that the velocity vector be rotated toward the south in the orbit plane. But this rotation in turn required that the position vector at periapsis be rotated south, reducing the latitude of the periapsis vector. A value for ϕ_p of 18.5 deg would reduce the angle of attack to the 25 deg needed by the RPA.

Recall that the preflight VOI maneuver strategy was a 3×3 search, using three controls to achieve three specified parameters. Now we have four target requirements. Hence, the problem is that we have more target conditions than controls at VOI. However, TCM3 provides three additional controls, one of which was used to correct errors in the time of arrival at Venus, leaving two for changing B and θ in the B plane at Venus. The method of solution is, therefore, to select a new aimpoint (if one exists) that achieves all four specified values in the absence of errors.

Method of Locating New Aimpoint

The curves in Fig. 2 can now be used to generate contours of constant ϕ_p for the acceptable targeting region in Fig. 1. A horizontal line drawn across Fig. 2 at $\phi_p = 18.5$ deg shows which values of B and θ would produce all four specified values. The contour for $\phi_p = 18.5$ deg is sketched in Fig. 1 and any point along this curve that is inside the acceptable targeting region would satisfy our current problem. Determining other contours of constant ϕ_p in a similar manner shows that, in general, the value of the achieved celestial latitude of the periapsis vector increases (or decreases) as the approach trajectory is moved up (or down) in the region of Fig. 1

This curve in B, θ space was available because we added two controls to the targeting process to achieve one additional targeting condition. The final aimpoint was selected along this curve to provide a real-time backup ignition time feature. The orbit insertion maneuver was executed by stored commands in the two onboard command processors.[5] If the VOI engine had failed to ignite at the nominal burn time, a series of stored backup commands to fire would have been used. In addition, a backup feature involving the sending of real-time ignition commands was also desired. Since the spacecraft would be occulted from Earth view during the burn, the real-time command would be timed to arrive repeatedly at the spacecraft beginning when it emerged from Earth occultation. (The idea of sending a real-time backup command to ignite immediately after Earth occultation was originally suggested by C.F. Hall, the Pioneer Venus Project Manager.) Late ignition would, of course, alter the targeted orbit characteristics but could provide useful orbit conditions.

To enhance the effect of a real-time command ignition, the objective was to select a VOI maneuver whose orientation would be as close as possible to the orientation of the negative

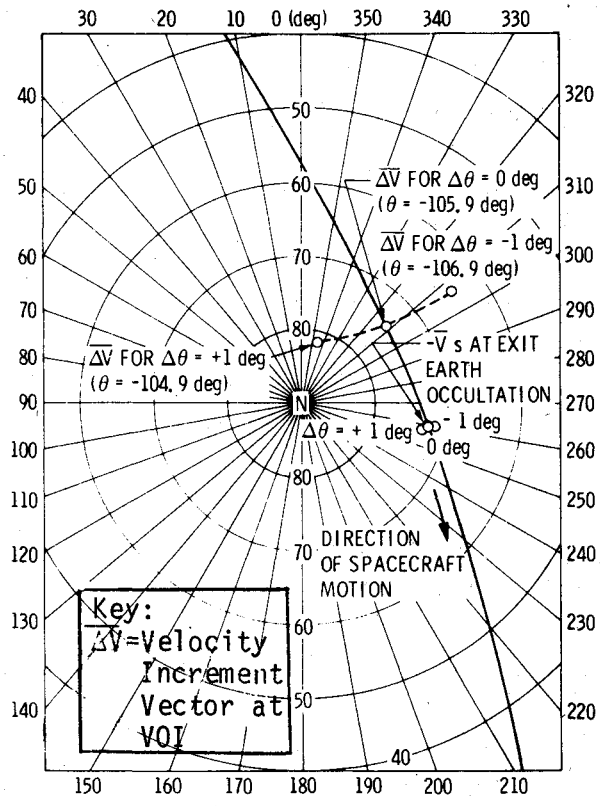

Fig. 4 Geometric picture for real-time VOI ignition command analysis.

velocity vector of the spacecraft as it exited Earth occultation. The geometric picture is shown in Fig. 4, which includes the negative velocity vector as the spacecraft exited Earth occultation† and maneuver directions for each of the three aimpoints corresponding to $\Delta\theta = -1.0$, 0.0, and 1.0 deg on the $\phi_p = 18.5$ deg contour. The second of these aimpoints ($\Delta\theta = 0.0$ deg) would produce the smallest angle and, hence, the most efficient maneuver.

This fact was checked numerically by simulating the maneuver for each of these three cases at the exit occultation point, i.e., at the same nominal orientation and ΔV magnitude but at the later time to determine the resulting orbit elements. The achieved values for the period would have been 54, 49, and 56 h, respectively. By using only 4 m/s the 49-h period produced by the in-plane VOI could be adjusted to 48 h, thus synchronizing the spacecraft with respect to the ground station on alternate Earth days. There was not enough liquid fuel onboard the spacecraft to decrease the period from 49 to 24 h.

The real-time command at the end of the occultation would have produced a dangerously low periapsis altitude of 180 km; the large period, however, would have provided ample time to perform a maneuver to raise the closest approach distance. The characteristics of the resulting orbit were considered acceptable for a backup maneuver; therefore, the second aimpoint listed above ($\Delta\theta = 0$ deg) was selected (see Table 1, column 3).

Recall that we have always used the first intersection point between the pre- and post-VOI trajectories. For a maneuver at either point, there had to be a nonzero angle between the $\overline{V}$ and $\overline{\Delta V}$ because there was more than enough ΔV available to reduce the energy to that of a 24-h orbit. For the first intersection point, this angle was formed by having the $\overline{\Delta V}$ ahead of the $-\overline{V}$ in the orbit plane; for the second, the reverse

†The value used for the Venus radius in computing distances above the planet surface is 6052 km. A radius of 6139 km was used to account for occultation by the Venus atmosphere which was modeled as being geometric in this analysis.

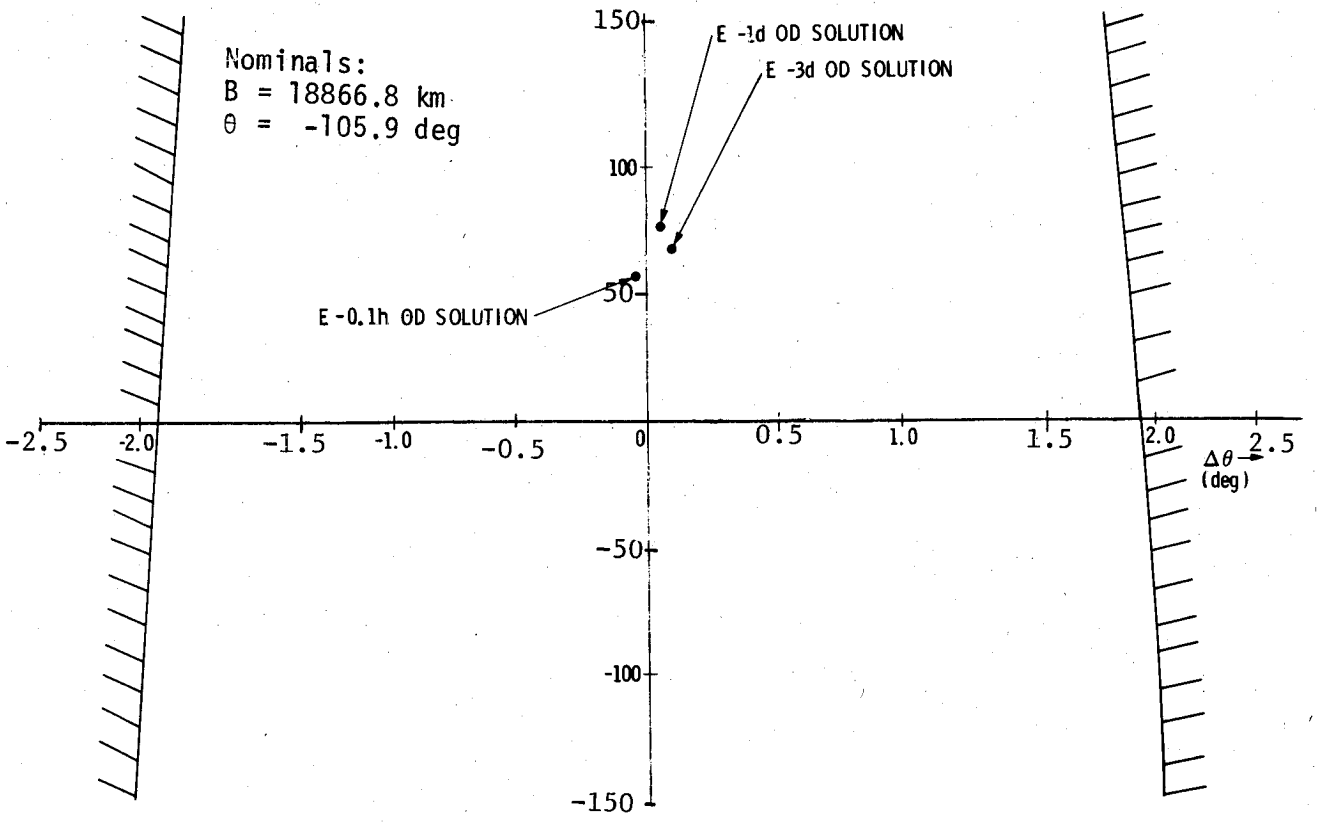

Fig. 5 Acceptable targeting region in the B plane for the in-flight VOI strategy.

relationship was true. As a result, the maneuver for the first intersection was more efficient at exit occultation when the real-time command could be initiated than that for the second. Therefore, the second point was rejected to provide a better real-time backup capability.

In-Flight Venus Orbit Insertion Strategy

The new aimpoint at Venus is given in Table 1. The last interplanetary trajectory correction maneuver targeted the spacecraft to approximately this new aimpoint on Nov. 2, 1978, 32 days before Venus encounter, for only 0.2 m/s. An offset of 35 km was introduced into this targeting to account for the B-plane change that would be produced at E – 2d when the spacecraft was turned to the direction required for the orbit insertion maneuver. This offset also anticipated the change caused by increasing the spin rate to 52 rpm for attitude stability during the VOI burn.

However, orbit determination and execution errors incurred at TCM3 produced an arrival point other than the desired one. The principal uncertainty here was the OD experienced in determining the trajectory for use in calculating the TCM3 maneuver parameters.

After the implementation of TCM3, only the three controls of the VOI maneuver were available to correct errors. The VOI strategy used was to target to period, inclination, and ϕ_p, leaving post-TCM3 dispersions affecting h_p to be corrected in orbit. These h_p dispersions were dominated by the OD errors experienced when TCM3 was designed. The uncertainty in the state at E – 3d when the VOI maneuver was determined and the VOI execution errors were the principal sources of inaccuracy for period and ϕ_p. Errors in i reflect the OD uncertainty in determining the direction perpendicular to the B vector at E – 3d. The resulting orbit accuracy was considered acceptable. A specific requirement was to have $h_p > 200$ km on the initial orbit. Given a target h_p of 350 km and 1σ control in h_p of 37 km, it was 99% probable that h_p would be greater than 264 km (assuming a one-dimensional normal distribution in h_p in the calculation of this estimate).

Method of Determining VOI Parameters

Figure 5 reflects the in-flight VOI strategy in that it gives the region in the B plane from which the spacecraft can be inserted into an elliptic orbit having the specified values for period, inclination, and ϕ_p. This figure corresponds to Fig. 1 for the original orbit insertion strategy. Note that the parameters given along the axes are deltas from the new aimpoint (third column of Table 1) in B vs θ space.

Figure 6 gives the contours for the achieved periapsis altitude that correspond to vertical slices in this region in the arrival space. Figure 7 provides similar data for the celestial latitude of the spacecraft $\overline{\Delta V}$. Contours for other nontargeted orbit elements, the remaining spacecraft controls, ELA, SLA, and other trajectory data were also generated.

After the last TCM, the OD process determined the achieved trajectory that was mapped to the B space at Venus. As each OD was obtained, the resulting (B,θ) point was checked to see if it fell within the acceptable targeting region of Fig. 5. If the OD estimate had never moved into this region, a late TCM would have been needed. Since the estimate did fall within this region, the contours could be used to redesign the VOI maneuver on paper. That is, the spacecraft controls (the time of ignition and the two orientation parameters) were determined by interpolating between the contours above and below the $\Delta\theta$, that is, the achieved θ minus the aimpoint θ value. The interpolation was done at the ΔB that is the achieved B minus the aimpoint B value. The resulting $\overline{\Delta V}$ was then checked against pointing constraints by comparing its orientation to Fig. 3 and checking the ELA, SLA, and distance at closest approach contours at the estimated $(\Delta B,\Delta\theta)$ point for satisfying their constraints.

Note that if the spacecraft had been targeted to P, h_p, and i at the new aimpoint, the ϕ_p would have been very sensitive to the delivery errors at the planet. Figure 2 shows that for an approach trajectory near $\Delta B = -108$ km and $\Delta\theta = 0.0$ deg a delivery error of 50 km, i.e., about 1σ, in B would produce a 2.5 deg error in ϕ_p. However, as shown in Fig. 6, targeting to period, inclination, and ϕ_p would produce only a 30 km error

Table 2 Nominal sensitivities for the VO maneuver

	Period, min	Periapsis altitude, km	Inclination, deg	Latitude of periapsis, deg
B, km	0.3	0.6	0	0.002
θ, deg	0	0	−1.0	0.17
Linearized time of flight, s	1.7	0.3	0	−0.01
Time of ignition, s	−1.7	−0.3	0	0.01
Celestial latitude of $\overline{\Delta V}$, deg	10.2	0.6	0.1	0.08
Celestial longitude of $\overline{\Delta V}$, deg	−7.9	−0.5	0.01	−0.06
ΔV, m/s	−4.9	0.02	0	0.002

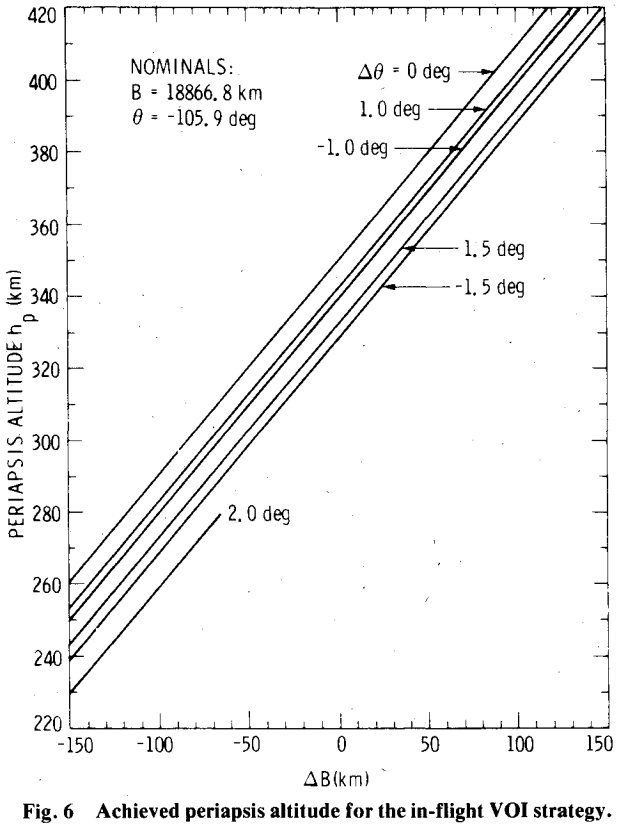

Fig. 6 Achieved periapsis altitude for the in-flight VOI strategy.

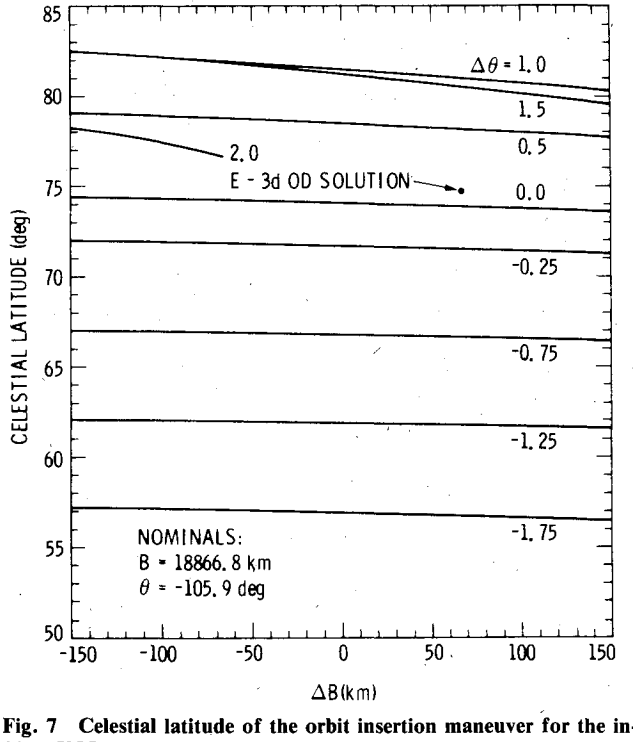

Fig. 7 Celestial latitude of the orbit insertion maneuver for the in-flight VOI strategy.

in h_p. A 2.5 deg error in ϕ_p would cost more than 78 m/s to correct in orbit, while 30 km in h_p could be corrected for about 2 m/s. Of course, less ΔV is usually needed to change h_p than out-of-plane parameters such as ϕ_p.

Before the final commands were sent to the spacecraft, a high-precision numerical-search computer program was used to fine tune the controls. In this process, the values obtained from the contours for the spacecraft controls were used as initial guesses for the search to avoid convergence problems and reduce computer running time and costs.

Real-Time Updates and Results

Sensitivity Data

Table 2 provides sensitivities of the elliptic orbit elements to variations about the nominal approach trajectory and VOI maneuver parameters (Table 1, column 3). For example, as mentioned in the above discussions, $\partial h_p/\partial B = 0.6$. Note, in particular, that this table adds sensitivity information for the VOI execution errors and for the approach trajectory in the direction normal to the B plane.

Real-Time Adjustments

At this point, the expected performance of the solid rocket was reassessed and the ΔV was predicted to be 1.1007 km/s, an increase of 2.5 m/s. Also, the target value for period was biased to be 13.8 min smaller than desired because reducing this parameter in orbit would require use of an operationally complex thruster. The bias would decrease the size of a trim needed to correct a positive dispersion. The best estimate approach trajectory available at E − 3d (Table 3) was then used to determine the required VOI maneuver parameters.

The 3 × 3 search to the new period used the new ΔV and OD estimates, but Table 2 demonstrates essentially what happened. The celestial latitude and longitude of the ΔV were essentially as predicted by the contours for $\Delta B = 67$ km and $\Delta\theta = 0.1$ deg (see Fig. 7). The target change for period of −13.8 min was nearly provided by the 12.3 min reduction caused by the increased ΔV. The update in the OD estimate for time of closest approach (TCA) on the hyperbolic trajectory required a one-for-one changer in the time of ignition. Hence, the value of t_{ign} was merely adjusted by

$$\Delta t_{ign} = \frac{P(\text{target change}) - P(\Delta V \text{ change})}{\partial P/\partial t_{ign}} + \Delta\text{TCA} \qquad (1)$$

At E − 2d, the spacecraft was turned to the VOI attitude. After one attitude-refining turn, the partials with respect to orientation were used to show that no further adjustments were necessary. The only elliptic parameter that was significantly affected by small orientation errors was period. The ignition time, which could still be updated in the onboard

Table 3 Maneuver updates for revised encounter conditions at Venus

Parameters	Orbit determination solutions		
	E − 3d[a]	E − 1d[a]	E − 0.1 h
B, km	18,933.7	18,943.2	18,923.7 ± 1.1 (1σ)
θ, deg	−105.8	−105.9	−106.0 ± 0.02 (1σ)
TCA on 12-04-78 (UTC at spacecraft), h:min:s	16:00:03.4	16:00:07.3	16:00:03.6 ± 0.07 s (1σ)
Celestial latitude of $\overline{\Delta V}$, deg	74.76	74.85	[b]
Celestial longitude of $\overline{\Delta V}$, deg	316.82	316.10	[b]
Time of ignition on 12-04-78 (UTC at spacecraft), h:min:s	15:58:05.4	15:58:17.5	[b]

[a] Expected effects for the VOI turn and spinup have been included.
[b] No maneuver was computed for the E − 0.1 h state estimate.

Table 4 Orbit elements and uncertainties

Parameters[a]	Uncertainties from premaneuver OD (1σ)	In-orbit solution ±1σ	Original achieved orbit parameters	Adjusted orbit parameters	Deltas
Period, h:min:s	0.5 min	3:11:23.2 ± 1.6 s	23:11:23.2	23:11:23.2	0.0
Periapsis altitude, km	0.7	379.28 ± 0.15	380.37	379.28	0.0
Inclination, deg	0.02	105.05 ± 0.08	105.16	105.16	0.11
Longitude of ascending node, deg	0.01	22.78 ± 0.09	22.77	22.77	−0.01
Argument of periapsis, deg	0.002	160.67 ± 0.02	160.69	160.69	0.02

[a] The period value is the osculating value at the first apoapsis. All other parameters correspond to the state at 16 h:30 min:00 s UTC on Dec. 4, 1978.

computer, also significantly changed only this parameter. So the known errors in the orientation could be compensated for by modifying t_{ign}.

On Dec. 3, 1978, the spin rate was increased to 52 rpm to provide orientation stability during the VOI burn. As the spacecraft approached the planet, additional OD estimates for the trajectory were obtained. The sensitivities in Table 2 were used to determine any required updates to the stored onboard commands. Recall that the perturbations in arrival space caused by the pre-VOI turns and spinrate change were anticipated in the targeting at TCM3, but variations from the nominal perturbations were inevitable and were accounted for by modifying the time of ignition command.

Using the OD estimate at E − 1d, an update for the expected orientation at VOI, and an additional bias (ΔP_T) in the period specification, a new Δt_{ign} was computed as

$$\Delta t_{ign} = \left(-\Delta\phi_{\Delta V}\frac{\partial P}{\partial \phi_{\Delta V}} - \Delta\lambda_{\Delta V}\frac{\partial P}{\partial \lambda_{\Delta V}} + \Delta\mathrm{TCA} - \Delta B\frac{\partial P}{\partial B} - \Delta\theta\frac{\partial P}{\partial \theta} + \Delta P_T\right)\Big/\frac{\partial P}{\partial t_{ign}} \quad (2)$$

The adjusted t_{ign} was then fine tuned via a high-precision numerical search program to obtain the value sent in the command update at E − 1d. The important fact here, observed in Table 2, is that all of the perturbations in Eqs. (1) and (2) affect only period and this parameter could be corrected by adjusting t_{ign} without significantly changing other orbital elements.

Reconstruction of the VOI Maneuver

After the E − 1d maneuver update, the interplanetary OD team continued estimating the pre-VOI trajectory, obtaining the last solution given in the third column of Table 3 with 1σ statistical values. These uncertainties were also mapped linearly through the nominal burn to obtain the variations given in the first column of Table 4. The orbit insertion was performed on Dec. 4, 1978. In-orbit elements were then determined by the satellite OD team from data taken after VOI (Table 4, column 2). Estimates for the actual (as performed) VOI maneuver parameters were then obtained by requiring the maneuver to match the pre- and postinsertion OD solutions.

The method used was:

1) Target a 1 × 1 maneuver simulation (VOI ΔV to the achieved period), using the average spacecraft orientation during the burn. Average orientation parameters were acceptable because the attitude was very stable. This step treats the premaneuver OD solution as being perfect and accumulates all errors in the achieved elements (Table 4, column 3). This process indicated an overburn of 6.4 m/s.

2) Adjust the pre-VOI solution within the given dispersions. In this step, the principal source of the 1.1 km error in periapsis altitude (Table 4, column 3) is isolated as follows. This delta must be caused by the three error sources: interplanetary OD, VOI execution errors, and in-orbit OD. However, execution errors could not affect h_p because the VOI was performed near periapsis (see partials of h_p with respect to ΔV, $\phi_{\Delta V}$, and $\lambda_{\Delta V}$). Also, the in-orbit OD uncertainty in h_p was only 0.15 km (1σ). Therefore, we must adjust the pre-VOI OD estimate by

$$\Delta B = \frac{\Delta h_p}{\partial h_p/\partial B} = 1.8 \text{ km}$$

3) Refine the maneuver ΔV. Since the premaneuver B value was actually $\Delta B = 1.8$ km less than that given in the last column of Table 3, even the nominal VOI would have produced a period that was

$$\Delta P = \Delta B \partial P/\partial B = 0.5 \text{ min}$$

less than expected. Therefore, the amount of overburn was

$$|\Delta\Delta V| = \frac{\Delta P}{|\partial P/\partial \Delta V|} = 0.1 \text{ m/s}$$

less than that obtained in step 1, i.e.,

$$\Delta V = 1.1070 \text{ km/s}$$

4) Adjust the in-orbit parameters accordingly, using the partial derivatives, to produce the values given in the fourth column of Table 4.

Table 5 Reconstructed orbit insertion maneuver parameters

Maneuver parameter	Commanded value	Estimated actual value	Error	A priori 1 σ	Error level
Increment magnitude (ΔV), m/s	1100.7	1107.0	+6.3	2.2	2.9σ
Celestial latitude of $\overline{\Delta V}$, deg	74.76	79.93 (avg)	Pointing error, deg		
Celestial longitude of $\overline{\Delta V}$, deg	316.82	316.51 (avg)	0.19	0.24	0.8σ
Time of ignition on 12-04-78 (UTC at spacecraft), h:min:s	15:58:17.5	15:58:17.5	0	...	...

5) Verify this process via a high-precision 1×1 numerical search, using the initial conditions in Table 3, column 3, less 1.8 km in B. This step obtained the maneuver in Table 5 and the orbital elements in the fourth column of Table 4.

6) Interpret the results statistically. The orbiter experienced a 6.3 m/s ($0.57\% = 2.9\sigma$) overburn. Since the average orientation was at an angle of about 0.19 deg to the commanded direction, pointing errors were about 0.8σ.

Thus, an estimate for the VOI maneuver parameters was determined which matched the pre- and post-VOI trajectories to within the uncertainties of the OD statistics.

Concluding Remarks

This paper describes methods that are suitable for hand computations to: 1) determine the required aimpoint at a target body and the associated nominal orbit insertion maneuver parameters (controls) for obtaining specified elliptic orbit values; 2) modify the orbit insertion controls to account for delivery errors remaining after the last interplanetary trajectory correction; 3) adjust these controls in the real-time flight operations environment to account for orbit determination updates, known spacecraft orientation errors, and changes in a target specification; and 4) reconstruct the actual (as performed) orbit insertion maneuver parameters after execution.

The aimpoint selection process and orbit insertion maneuver strategy provided four target elliptic elements to within satisfactory accuracies, an acceptable arrival time at the planet, and backup ignition time capability. They also conserved orbiter fuel where possible and satisfied attitude control, communication, and hardware pointing constraints. The maneuver update process is rapid and the reconstruction method is simple. All of these methods add to the analyst's understanding of the interplanetary targeting and orbit insertion problems. Therefore, they should be useful in the navigation of future spacecraft missions for planetary exploration.

Acknowledgments

The research described in this paper was carried out at the Jet Propulsion Laboratory, California Institute of Technology, under Contract NAS7-100 sponsored by NASA. The Pioneer Venus Project is managed for NASA by the Ames Research Center. One of the Jet Propulsion Laboratory responsibilities is navigation support, including maneuver analysis. The author acknowledges the expert computer programming of E.A. Rinderle Jr. and B.L. Paulson for software used in these analyses.

References

[1] Dyer, J.W., Nunamaker, R.R., Cowley, J.R. Jr., and Jackson, R.W., "Pioneer Venus Mission Plan for Atmospheric Probes and an Orbiter," *Journal of Spacecraft and Rockets,* Vol. 11, Oct. 1974, pp. 710-715.

[2] Cowley, J.R. Jr., "Orbit Selection for the 1978 Pioneer Venus Mission," AIAA Paper 76-798, San Diego, Calif., Aug. 1976.

[3] Shapiro, I.I., Reasenberg, R.D., Hintz, G.R., Jacobson, R.A., Kirhofer, W.E., and Wong, S.K., "Venus: Density of Upper Atmosphere from Measurements of Drag on Pioneer Orbiter," *Science,* Vol. 203, No. 4382, Feb. 23, 1979, pp. 775-777.

[4] "Pioneer Program Trajectory Characteristics for Orbiter Mission," NASA Ames Research Center, Moffett Field, Calif., Doc. No. PT-402, Sept. 13, 1976.

[5] Barker, F.C. et al., "Pioneer Venus Orbiter Spacecraft Mission Operational Characteristics Document," Hughes Aircraft Co., PC-402, Feb. 1978.